Determination of the Fe magnetic anisotropies and the CoO frozen spins in epitaxial CoO/Fe/Ag(001)

J. Li,[1] Y. Meng,[1] J. S. Park,[1] C. A. Jenkins,[2] E. Arenholz,[2] A. Scholl,[2] A. Tan,[1] H. Son,[1] H. W. Zhao,[3] Chanyong Hwang,[4] Y. Z. Wu,[5] and Z. Q. Qiu[1,*]

[1]*Department of Physics, University of California at Berkeley, Berkeley, California 94720, USA*
[2]*Advanced Light Source, Lawrence Berkeley National Laboratory, Berkeley, California 94720, USA*
[3]*Institute of Physics, Chinese Academy of Science, Beijing, 100190, P.R. China*
[4]*Korea Research Institute of Standards and Science, Yuseong, Daejeon 305-340, Korea*
[5]*Department of Physics, Fudan University, Shanghai, P.R. China*

(Received 28 April 2011; revised manuscript received 17 August 2011; published 28 September 2011)

CoO/Fe/Ag(001) films were grown epitaxially and studied by X-ray Magnetic Circular Dichroism (XMCD) and X-ray Magnetic Linear Dichroism (XMLD). After field cooling along the Fe[100] axis to 80 K, exchange bias, uniaxial anisotropy, and 4-fold anisotropy of the films were determined by hysteresis loop and XMCD measurements by rotating the Fe magnetization within the film plane. The CoO frozen spins were determined by XMLD measurement as a function of CoO thickness. We find that among the exchange bias, uniaxial anisotropy, and 4-fold anisotropy, only the uniaxial magnetic anisotropy follows thickness dependence of the CoO frozen spins.

DOI: 10.1103/PhysRevB.84.094447 PACS number(s): 75.70.Ak

I. INTRODUCTION

Exchange bias[1] in ferromagnetic (FM)/antiferromagnetic (AFM) systems has been one of the most intensely studied topics in nanomagnetism research because of its importance to spintronics technology.[2] While it is well acknowledged that it is the AFM layer that induces the exchange bias,[3] it remains a mystery on how the induced exchange bias and other types of magnetic anisotropies in the FM layer depend on the specific AFM spin configurations. Early theories were aimed to single out the physical origin of the exchange bias by using over-simplified AFM spin structures.[4–7] These models were soon replaced by more sophisticated models that are believed to better represent realistic experimental systems.[8–10] In many experiments, most of the early measurements are on the FM-layer hysteresis loops to study the pinning effect,[11–13] training effect,[14–16] and finite-size effect,[17,18] etc. One important issue in these studies is how the AFM/FM interfacial coupling determines the FM-layer exchange bias and the magnetic anisotropies. Doping the AFM layer with nonmagnetic elements[19–21] and studying a FM/AFM/FM trilayer[22] show that the exchange bias is influenced by the AFM bulk-spin structure, although the direct FM/AFM interaction comes from the interface. Recognizing that measurement on the FM layer provides only indirect information on the AFM spins during the FM-magnetization reversal, X-ray Magnetic Circular Dichroism (XMCD) and X-ray Magnetic Linear Dichroism (XMLD)[23] have recently been applied to measure both the FM and the AFM layers using element-specific measurements. XMCD measurement shows that there exists a small amount of uncompensated spins in the AFM layer,[24] and that only a small percentage of the uncompensated spins is pinned to account for the exchange bias.[25–28] Furthermore it is found that these pinned uncompensated AFM spins actually extend into the AFM layer,[29] supporting the FM-layer measurement result that the whole AFM layer matters to the exchange bias. This result suggests that the AFM-spin structure during the FM-layer magnetization reversal is very important to the AFM-induced exchange bias and magnetic anisotropies in the FM layer. Recently, XMLD was applied to directly probe the AFM-compensated spins during the FM-layer magnetization reversal.[30] The result shows that there exists two types of CoO spins in the Fe/CoO system with respect to the Fe-magnetization change: rotatable spins and frozen spins. Although it is expected that the rotatable spins occur at thinner CoO thickness and the frozen spins occur at thicker CoO thickness, it is surprising that neither the exchange bias nor the coercivity of the Fe film follows the amount of frozen spins in the CoO layer.[31] This discovery suggests that the induced exchange bias and the magnetic anisotropies come from different origins of the AFM spins. In fact it has been noticed that the exchange bias and the magnetic coercivity of the FM layer have very different and complicated dependence on the AFM-layer thickness,[31,32] on the spacer layer between the FM and AFM layers,[33] and on the temperature.[34] The interesting question is this: How do the rotatable and frozen CoO spins determine the different types of magnetic anisotropies and specifically which type of magnetic anisotropy is directly correlated to the frozen spins of the CoO layer? A clarification of this issue obviously requires a separation of different types of the magnetic anisotropies in experiment so that it is possible to compare each of the anisotropies with the frozen spins in the AFM layer. In this paper we report an experimental study of CoO/Fe/Ag(001) single crystalline thin films. Using XMLD measurements within a magnetic field parallel and perpendicular to the field cooling direction, we are able to separate the rotatable and frozen spins in the CoO layer. Using XMCD measurements with a magnetic field rotating within the film plane, we are able to separate the exchange bias (unidirectional), uniaxial, and the 4-fold magnetic anisotropies of the Fe film. We find that only the uniaxial magnetic anisotropy follows the CoO frozen spins.

II. EXPERIMENT

A Ag(001) single-crystal substrate was cleaned in an ultra-high vacuum system by cycles of Ar ion sputtering at ∼2 keV

and annealing at 600 °C. A 20-monolayer (ML) Fe film was grown on top of the Ag(001) substrate at room temperature (RT). Then a CoO wedge (0–5 nm) was grown on top of the Fe film by deposition of Co under an oxygen pressure of 1×10^{-6} Torr. Low Energy Electron Diffraction (LEED) confirms the epitaxial growth of single crystalline CoO and Fe films on the Ag(001) substrate[31] above at least 1 nm CoO. As reported in the literature, Fe film on Ag(001) has a bcc structure with the Fe [100] axis parallel to the Ag [110] axis, and CoO film on Fe(001) has an fcc structure with the CoO [110] axis parallel to the Fe [100] axis. The sample is covered by a 2-nm Ag-protection layer and then measured at beam lines 4.0.2 at the Advanced Light Source (ALS) of the Lawrence Berkeley National Laboratory. The x-ray beam size at BL4 is 50–100 μm so that with the slope of 1 nm/mm in our sample we have a thickness resolution of 0.05–0.1 nm for results described in this paper. For the Fe XMCD measurements the x-ray beam was at an incident angle of 80° to the sample surface. We fixed the polarization of x ray to right circular polarization when taking the x-ray absorption spectrum (XAS). After dividing Fe L2-peak by L3-peak intensities, we get the XMCD signal and plot it as a function of applied magnetic field (in the x-ray incident plane) to obtain the Fe-magnetic hysteresis loop.

III. RESULTS AND DISCUSSION

The sample was cooled down to 80 K from RT within a 4000-Oe external magnetic field applied in the Fe in-plane [100] axis. The cooling field direction is in the film plane and could be either in or perpendicular to the x-ray incident plane. Figure 1 shows the Fe-magnetic hysteresis loops taken for magnetic field applied parallel to the field cooling Fe[100] direction and perpendicular to the field cooling direction (Fe[010] axis). The hysteresis loops for the magnetic field along these two directions are identical for CoO thickness (d_{CoO}) thinner than 1.5 nm and become different at d_{CoO} > 1.5 nm. As d_{CoO} increases to 4 nm, the Fe hysteresis loop is obviously an easy-axis loop with a full remanence for field parallel to the field-cooling direction, and a hard-axis loop with near zero remanence and a high saturation field for field perpendicular to the field-cooling direction. This characteristic of the hysteresis loops represents a magnetic system with a uniaxial magnetic anisotropy whose easy magnetization axis is along the field-cooling axis. Thus we conclude that the field cooling induces a uniaxial anisotropy to the Fe film at d_{CoO} > 1.5nm. The critical value of d_{CoO} = 1.5 nm must depend on temperature, as uniaxial anisotropy should obviously disappear above the CoO Néel temperature. Unfortunately our limited beam time will not allow us to do a temperature-dependent study. Fortunately a systematic temperature-dependent study on the anisotropies was already performed on a Co/FeF_2 system,[34] although XMLD cannot be applied to a FeF_2 layer. We also notice an exchange-bias field of 300 Oe in the d_{CoO} = 4.0 nm sample, which is quite similar to the value reported in the literature.[31] The hysteresis-loop result suggests that the AFM order of the CoO film after field cooling induces different Fe-film magnetic anisotropies at different CoO thicknesses. Recognizing the 4-fold symmetry of the CoO/Fe/Ag(001) system, the only possible effect of the CoO film during a field cooling in the Fe[100] direction is to generate an exchange bias (unidirectional anisotropy K_1), uniaxial anisotropy (K_2), and a 4-fold magnetic anisotropy (K_4), the hysteresis-loop result in Fig. 1 shows that the CoO AFM order after field cooling in the Fe[100] direction produces K_4 only in thin CoO thickness regime but produces all K_1, K_2, and K_4 in thick CoO regime. In a previous work we showed that the CoO spins consist of rotatable and frozen spins with respect to the Fe-magnetization rotation, the amount of the frozen spins increases with the CoO thickness, and the exchange bias is not directly correlated to the CoO frozen spins.[31] Then the interesting question is which of the K_1, K_2, and K_4 is directly correlated to the CoO frozen spins? To answer this question, we need to determine all K_1, K_2, and K_4 as a function of CoO thickness.

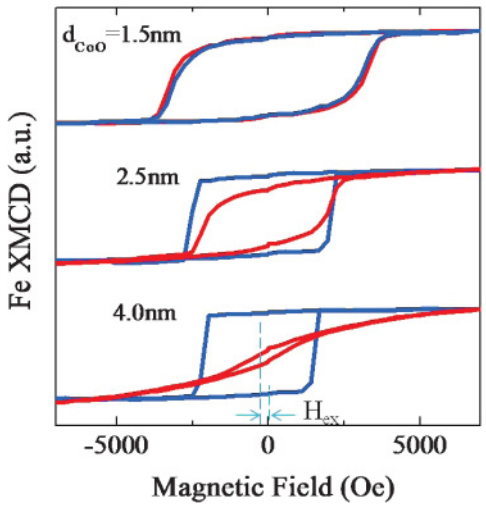

FIG. 1. (Color online) Fe hysteresis loops of CoO/Fe/Ag(001) at 80 K for field parallel (blue) and perpendicular (red) to the field-cooling direction of Fe[100]. The difference between the two loops for CoO thickness thicker than 2.5 nm shows the existence of a uniaxial magnetic anisotropy with the easy-magnetization axis parallel to the field-cooling direction.

While K_1 can be determined directly from the exchange bias of the hysteresis loop along the field-cooling direction and K_2 can be estimated from the saturation field of the hard-axis loop, the value of K_4 is not directly proportional to the coercivity of the hysteresis loop. One approach to determine the K_2 and K_4 values is to fit the hard-axis hysteresis loop by assuming a coherent rotation of the Fe magnetization during the saturation process.[34,35] The disadvantage of this method is that it does not apply to hysteresis loops involving domain formation during the magnetization reversal, especially to hysteresis loops with nonzero coercivity.

A better method to determine the magnetic anisotropy is to rotate the Fe magnetization within the film plane with a constant magnetic field and to determine the Fe-spin direction relative to the external magnetic field (in reality to determine the projection of the Fe spin onto a specific in-plane direction). This method is based on the principle of balancing the total magnetic torque exerted on the magnetic thin film[36] and has been successfully exercised in the Rotating-of-Field Magneto-Optic Kerr Effect (ROTMOKE)[37,38] and the measurement of angular dependent planar-Hall resistivity.[39,40] To illustrate how this method works, consider the energy of a magnetic thin film within an external magnetic field, which is strong enough to

bring the FM film into a single domain state,

$$E = -MH\cos(\theta_H - \theta) - MH_{\rm ex}\cos\theta + \tfrac{1}{2}MH_2\sin^2\theta + \tfrac{1}{2}MH_4\sin^2\theta\cos^2\theta. \quad (1)$$

Here H is the external magnetic field, θ_H and θ are the in-plane angles of the external magnetic field and the Fe magnetization with respect to the field-cooling direction, $H_{\rm ex} = K_1/M$ is the exchange-bias field, $H_2 = 2K_2/M$ is the uniaxial anisotropy field, and $H_4 = 2K_4/M$ is the 4-fold anisotropy field. Under this definition $H_2 > 0$ corresponds to a uniaxial anisotropy with the easy axis being the field-cooling direction, and $H_4 > 0$ corresponds to a 4-fold anisotropy with the easy axes being the Fe[±1,0,0] and Fe[0, ± 1,0] axes. Minimizing Eq. (1) with respect to θ leads to the balance of the external field torque and the internal anisotropy torque $l(\theta)$,

$$H\sin(\theta_H - \theta) = l(\theta) \equiv H_{\rm ex}\sin\theta + \tfrac{1}{2}H_2\sin 2\theta + \tfrac{1}{4}H_4\sin 4\theta. \quad (2)$$

Therefore, an experimental determination of the magnetization projection angle θ at each magnetic field angle θ_H will allow a determination of $H_{\rm ex}$, H_2, and H_4 by fitting the experimental curve using Eq. (2).

At beam line 4.0.2, the eight-pole magnet design[41] allows an element-specific XMCD measurement of the Fe magnetization by rotating a magnetic field within the film plane. Figure 2(a) shows the measurement geometry of our experiment. With the cooling-field direction perpendicular to the incident x-ray plane, we measured the projection of the Fe magnetization in the direction of incident x-ray beam ($I_{MCD} \propto \langle M\rangle \sin\theta$).[42,43] Thus the in-plane azimuthal angle of the Fe magnetization can be deduced from $\theta = \sin^{-1}(I_{MCD}(\theta)/I_{MCD}(90^\circ))$. Figure 2(b) shows the experimental data of $I_{\rm MCD}$ for a CoO(3nm)/Fe/Ag(001) sample as a function of the external field angle θ_H. The magnitude of the external field was fixed at 4000 Oe, which is sufficient to bring the Fe film into a single domain state. The maximum and minimum locations of the $I_{\rm MCD}$ occur at $\theta_H = 105^\circ$ and $\theta_H = 280^\circ$ rather than at $\theta_H = 90^\circ$ and $\theta_H = 270^\circ$, showing an appreciable difference between θ and θ_H, which is an indication of the existence of the magnetic anisotropy in the CoO/Fe/Ag(001). Figure 2(c) is the torque curve $l(\theta)$ as a function of the azimuthal angle (θ) of the Fe magnetization deduced from Fig. 2(b). By fitting the torque curve of Fig. 2(c) using Eq. (2) we determined the magnetic anisotropy constants $H_{\rm ex}$, H_u, and H_4. The fitting [red curve in Fig. 2(c)] agrees very well with the experimental data and yields the values of $H_{\rm ex} = 305 \pm 27$ Oe, $H_2 = 2184 \pm 39$ Oe, and $H_4 = -1997 \pm 89$ Oe. The XMCD measurement and fitting process are performed at different CoO thicknesses, and the result is shown in Fig. 3. The exchange-bias field obtained directly from the easy-axis hysteresis-loop measurement is also shown in Fig. 3. The $H_{\rm ex}$ obtained from the hysteresis loop agrees very well with the fitting result of $H_{\rm ex}$, showing the validity of using the fitting procedure to obtain $H_{\rm ex}$. To justify the values of the H_2 and H_4, we calculate the hard-axis hysteresis loops at $d_{\rm CoO} > 2.5$ nm (where the hard-axis character of the hysteresis loop becomes obvious) using Eq. (2) with the fitting values of $H_{\rm ex}$, H_2, and H_4 and $M/M_S = \sin\theta$. The calculated result is shown as the S curves (red solid lines) in Fig. 4. The segment of the S curve with negative H-M slope corresponds to a local high-energy state, which should lead to a jump of the magnetization giving rise to a nonzero coercivity.[35] The calculated curve (the segment of positive slope) agrees excellently with the experimental hysteresis loops, adjusting the method of fitting procedure for H_2 and H_4 as well as the method of obtaining H_2 and H_4 by fitting the hard-axis hysteresis loop exercised in Ref. 34.

Although CoO AFM order during the field cooling induces $H_{\rm ex}$, H_2, and H_4, their different $d_{\rm CoO}$ dependences (Fig. 3) show that the CoO spins induce these three quantities differently. It is also interesting to notice that the 4-fold anisotropy of the Fe film (H_4) undergoes an orientation transition with increasing

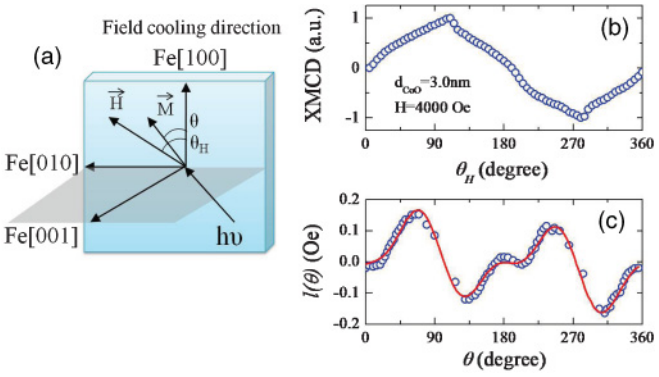

FIG. 2. (Color online) (a) Schematic drawing of the XMCD measurement. (b) The Fe XMCD signal, which is proportional to $M\sin\theta$ as a function of the field rotation angle θ_H. (c) The torque $l(\theta) = H\sin(\theta_H - \theta)$ deduced from (b) as a function of the Fe-magnetization angle θ. The red curve is the fitting result using Eq. (2).

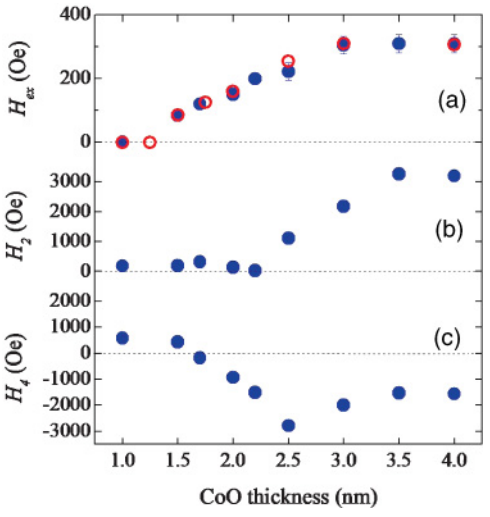

FIG. 3. (Color online) Fitting result of the (a) exchange-bias (unidirectional) field $H_{\rm ex}$, (b) uniaxial field H_2, and (c) the 4-fold anisotropy field H_4, as a function of the CoO thickness in CoO/Fe/Ag(001). Red circles in (a) are the result directly from the easy-axis hysteresis loop measurement. It is obvious that $H_{\rm ex}$, H_2, and H_4 depend differently on the CoO film thickness.

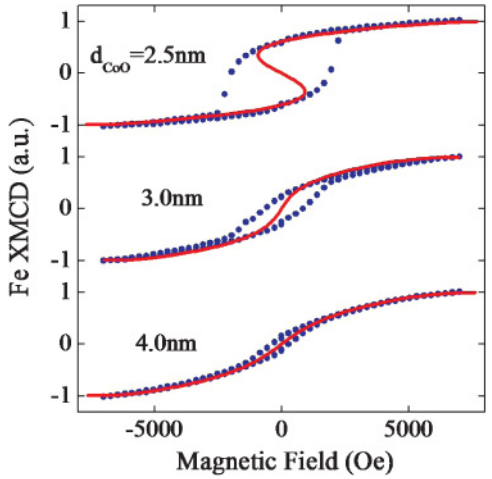

FIG. 4. (Color online) Calculated hard-axis hysteresis loops (red curves) from the fitting parameters of Fig. 3. The agreement between the calculated curves and the experimental data adjusts the validity of the fitting method.

the CoO thickness: the Fe easy axis of the 4-fold anisotropy is along the Fe[±1,0,0] and Fe[0, ±1,0] axes ($H_4 > 0$) in the thinner regime of the CoO film and switches to the Fe[±1,±10] axes ($H_4 < 0$) in thicker CoO regime. The switching of the 4-fold anisotropy easy axis in AFM/FM system was also reported in other AFM/FM systems[44–46] and was attributed to the interfacial spin frustration.

The different dependences of the H_{ex}, H_2, and H_4 on the CoO thickness indicate that they come from different mechanisms of the CoO/Fe interaction. To further explore the origin of the magnetic anisotropy induced by the CoO AFM order in the CoO/Fe/Ag(001), we performed the XMLD measurement on the CoO film by taking the XAS at the Co L_3 edge (Fig. 5) at normal incidence of the x-ray to the film. The L_3 ratio R_3 (defined as the ratio of the XAS intensity at 777.1 eV and 778.0 eV) is used to quantify the

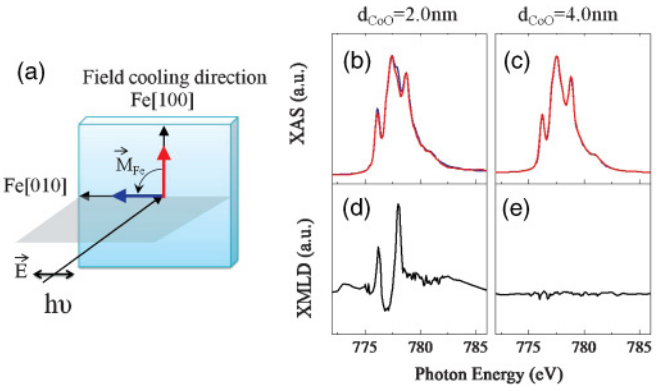

FIG. 5. (Color online) (a) Schematic drawing of the XAS measurement. The XAS of samples of CoO/Fe/Ag(001) for (b) d_{CoO} = 2 nm and (c) d_{CoO} = 4 nm. Red color spectrum is for Fe spin in the Fe[100] field-cooling direction, and blue color spectrum is for Fe spin in the Fe[010] direction. (d) The difference between the two XAS in (b) shows that CoO spins are rotatable in the d_{CoO} = 2.0 nm sample. (e) The identical XAS in (c) shows that CoO spins are frozen in the d_{CoO} = 4.0 nm sample.

XMLD effect.[47] Figure 5(a) and 5(b) present the XAS for CoO(2nm)/Fe/Ag(001) sample and the corresponding XMLD spectrum. The R_3 value is higher at $\vec{E} \perp \vec{M}_{Fe}$ than at $\vec{E} // \vec{M}_{Fe}$, where $\vec{E}$ is the x-ray polarization vector showing that the CoO spins are coupled perpendicularly to the Fe spins.[31] As the x-ray polarization $\vec{E}$ is fixed to the Fe[010] axis and the Fe magnetization is rotated by a 4000-Oe external magnetic field from the Fe[100] to Fe[010] direction, the nonzero XMLD signal shown in Fig. 5(b) indicates that the CoO spins also rotate with the Fe-spin rotation, i.e., the CoO spins are rotatable in this sample. In contrast the XAS of the CoO(4nm)/Fe/Ag(001) sample remains unchanged as the Fe spin switches from the Fe[100] to the Fe[010] direction, showing that the CoO spins in this sample are fixed to the crystal axis and do not follow the rotation of the Fe spin. In other words the CoO spins are frozen in the d_{CoO} = 4 nm sample. We define $\Delta R_3 = (R_3^{\perp} - R_3^{\parallel})/(R_3^{\perp} + R_3^{\parallel})$ to quantify the amount of rotatable/frozen CoO spins, where $R_3^{\perp}$ and $R_3^{\parallel}$ specify the L_3 ratio at $\vec{E} \perp \vec{M}_{Fe}$ and $\vec{E} // \vec{M}_{Fe}$, respectively. With this definition ΔR_3 should be proportional to the amount of rotatable CoO spins and reach its maximum value at 100% rotatable spins and minimum value at 100% frozen spins. It should be mentioned that although XMLD measurement in our experiment is a surface-sensitive technique, our previous result shows that the measurement under our given condition can probe at least 6-nm-thick CoO[31] to justify our method in determining the CoO frozen spins. Also 100% frozen spins here should really mean no detectable spins within the experimental error. From our previous experimental result (Ref. 31) our experimental sensitivity is ~0.5 ML. Figure 6(a) shows the result of ΔR_3 as a function of CoO thickness from which the percentage of the CoO frozen spins are deduced and shown in Fig. 6(b). The CoO spins are completely rotatable at d_{CoO} < 2 nm, partially frozen at 2.2 nm < d_{CoO} < 3.5 nm, and completely frozen at d_{CoO} > 3.5 nm. This result is consistent with our previous result.[31] By comparing the results of Fig. 3 and Fig. 6, it is easy to realize that only the uniaxial anisotropy of the Fe film follows the

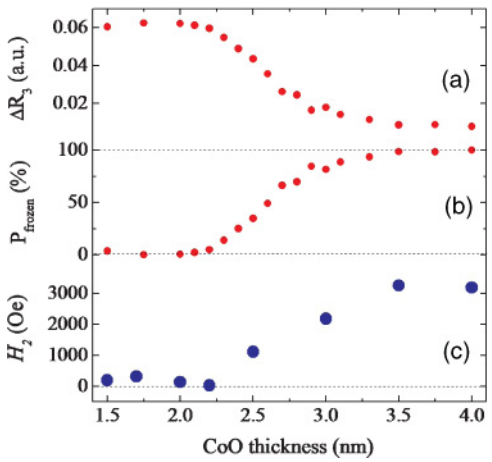

FIG. 6. (Color online) (a) The relative L_3 ratio difference (ΔR_3) as a function of the CoO thickness. (b) Percentage of the CoO frozen spins deduced from (a). (c) Uniaxial anisotropy field in Fig. 3(b) follows the CoO frozen spins.

frozen CoO spins in the CoO/Fe/Ag(001). To see this fact more clearly, we plot H_2 again in Fig. 6(c) to compare its d_{CoO} dependence with the CoO frozen spins. The similarity between Fig. 6(b) and Fig. 6(c) shows that the Fe-uniaxial anisotropy is proportional to the percentage of the CoO frozen spins: both of them start to appear at $d_{CoO} = 2.2$ nm and saturate at $d_{CoO} = 3.5$ nm. Therefore we conclude that the uniaxial anisotropy of the Fe film in CoO/Fe/Ag(001) is directly related to the CoO frozen spins. This result can be understood by the fact that only when the CoO spins are frozen due to the field cooling, the CoO spins are able to break the 4-fold symmetry of the CoO/Fe/Ag(001) system to generate a uniaxial (2-fold) anisotropy. In contrast if all CoO spins are completely rotatable, the CoO spins will follow the Fe-spin rotation so that they will not break the 4-fold symmetry of the system to generate a uniaxial anisotropy. From this mechanism the uniaxial anisotropy will be the energy needed to overcome the CoO/Fe interfacial coupling by rotating the Fe spin by 90° from the field-cooling direction. This scenario corresponds to the "spin-flop" mechanism in an antiferromagnet and has been proposed theoretically for the uniaxial magnetic anisotropy due to the AFM/FM interfacial interaction.[7] In experiment[48–50] the strength of the uniaxial anisotropy attributable to the AFM/FM coupling could vary from several tens of Oe in NiMn/Co[50] and NiO/Ni[51] to several hundreds of Oe in Fe/MnPd,[48] NiFe/NiO,[49] and Ni_81Fe_19/Cr_2O_3.[52] The strength of the uniaxial anisotropy in our CoO/Fe/Ag(001) system after field cooling is above 3000 Oe, which is much greater than the previous experimental data. This may be due to the epitaxial-growth nature of our sample and the strong CoO magnetic anisotropy ($\sim 2.7 \times 10^8$ erg/cm^3[53]). In fact a saturation field of $H_S = 3000$ Oe indicates a uniaxial anisotropy strength of $K_2 \approx M H_S d_{Fe}/2 \approx 0.7$erg/cm^2, which roughly agrees with the theoretical estimation 0.88 erg/cm^2 for a perfectly compensated interface.[54] To have a rough estimate of the CoO/Fe interfacial coupling strength, the uniaxial anisotropy from a perfect AFM/FM-compensated spin interface[7] can be easily deduced to be J_{FA}^2/J_A per spin, where J_{FA} and J_A refer to the AFM/FM interfacial interaction and the AFM exchange interaction, respectively. Then from the values of $K_2 \approx 0.7$erg/cm^2 and $J_A \approx k_B T_N \approx 25$ meV/spin $= 97$erg/cm^2, we estimate the CoO/Fe interfacial coupling strength to be $J_{FA} \approx \sqrt{J_A K_2} \approx 8$ erg/cm^2. It should be mentioned that the J_{FA} value estimated here is different from the "interfacial coupling" estimated from the exchange bias that has different definition and value ($J_{\text{int}} = H_{\text{ex}} M d_{\text{Fe}} \sim 0.01$–$0.1$ erg/cm^2). The latter actually represents an equivalent coupling between the FM layer and the uncompensated spins of the AFM layer.[2]

Figure 6 shows that the exchange bias and the 4-fold anisotropy are not correlated to the CoO frozen spins as closely as the uniaxial anisotropy. Although the exchange bias must come from the CoO AFM spin structure during the field cooling, H_{ex} already develops to 50–70% of its saturation value before the CoO film develops detectable frozen spins. In our previous work[31] we estimated that 5% CoO frozen spins are already responsible for $\sim 2/3$ of the exchange bias. There is no theoretical explanation yet on this fact and needs future investigation to fully understand the mechanism. Different from the exchange bias and the uniaxial anisotropies, a 4-fold magnetic anisotropy does not break the 4-fold rotation symmetry of the CoO/Fe/Ag(001) system so that frozen spins are not a necessary condition for the CoO to induce a 4-fold anisotropy. That explains why the Fe coercivity enhancement occurs at very thin CoO thickness where there is no exchange bias and uniaxial anisotropy and the CoO spins are completely rotatable. In fact a rotation of the CoO spins together with the Fe spins has to overcome not only the Fe anisotropy but also the CoO anisotropy.[55] The interesting observation of Fig. 3(c) is that the sign of the 4-fold anisotropy changes at $d_{CoO} = 1.7$ nm. We cannot associate this phenomenon with the CoO frozen spins because the H_4 does not follow the same thickness dependence of the CoO frozen spins. The sign change of the 4-fold anisotropy was reported in the FeMn/Co/Cu(001) system and was attributed to step-induced uncompensated spins at the AFM surface.[44–46] We do not know if the same mechanism accounts for the CoO/Fe/Ag(001) system. Further theoretical explanation is needed to explain our data.

IV. SUMMARY

In summary epitaxial CoO/Fe/Ag(001) films were grown and investigated using XMCD and XMLD after field cooling the sample to 80 K within an external magnetic field in the Fe[100] direction. We find that the CoO layer could induce unidirectional, uniaxial, and 4-fold anisotropies in the Fe film. Using XMCD measurement by rotating the Fe magnetization 360° within the film plane, we determine the dependence of the unidirectional, uniaxial, and the 4-fold anisotropies on the CoO thickness. XMLD was used to determine the amount of CoO frozen spins as a function of the CoO thickness. By comparing the magnetic anisotropies with the Co-frozen spins, we find that only the Fe uniaxial magnetic anisotropy is correlated with the CoO frozen spins.

ACKNOWLEDGMENTS

This work was supported by National Science Foundation DMR-0803305, US Department of Energy DE-AC02-05CH11231, KICOS through Global Research Laboratory project, and the National Natural Science Foundation of China.

*Corresponding author: qiu@socrates.berkeley.com

[1] W. H. Meiklejohn and C. P. Bean, Phys. Rev. **102**, 1413 (1956).
[2] J. Nogues and I. K. Schuller, J. Magn. Magn. Mater. **192**, 203 (1999).
[3] M. G. Blamire, M. Ali, C.-W. Leung, C. H. Marrows, and B. J. Hickey, Phys. Rev. Lett. **98**, 217202 (2007).
[4] N. C. Koon, Phys. Rev. Lett. **78**, 4865 (1997).
[5] D. Mauri, H. C. Siegmann, P. S. Bagus, and E. Kay, J. Appl. Phys. **62**, 3047 (1987).

[6] A. P. Malozemoff, Phys. Rev. B **35**, 3679 (1987).
[7] T. C. Schulthess and W. H. Butler, Phys. Rev. Lett. **81**, 4516 (1998).
[8] M. D. Stiles and R. D. McMichael, Phys. Rev. B **59**, 3722 (1999).
[9] P. Miltényi, M. Gierlings, J. Keller, B. Beschoten, G. Güntherodt, U. Nowak, and K. D. Usadel, Phys. Rev. Lett. **84**, 4224 (2000).
[10] M. Kiwi, J. Magn. Magn. Mater. **234**, 584 (2001).
[11] S. Maat, K. Takano, S. S. Parkin, and E. E. Fullerton, Phys. Rev. Lett. **87**, 087202 (2001).
[12] H. Ouyang, K.-W. Lin, C.-C. Liu, S.-C. Lo, Y.-M. Tzeng, Z.-Y. Guo, and J. van Lierop, Phys. Rev. Lett. **98**, 097204 (2007).
[13] X. P. Qiu, D. Z. Yang, S. M. Zhou, R. Chantrell, K. O'Grady, U. Nowak, J. Du, X. J. Bai, and L. Sun, Phys. Rev. Lett. **101**, 147207 (2008).
[14] T. Hauet, J. A. Borchers, Ph. Mangin, Y. Henry, and S. Mangin, Phys. Rev. Lett. **96**, 067207 (2006).
[15] S. Brems, K. Temst, and C. Van Haesendonck, Phys. Rev. Lett. **99**, 067201 (2007).
[16] S. K. Mishra, F. Radu, H. A. Dürr, and W. Eberhardt, Phys. Rev. Lett. **102**, 177208 (2009).
[17] K. Liu, S. M. Baker, M. Tuominen, T. P. Russell, I. K. Schuller, Phys. Rev. B **63**, 060403 (2001).
[18] J. Sort, A. Hoffmann, S.-H. Chung, K. S. Buchanan, M. Grimsditch, M. D. Baró, B. Dieny, and J. Nogués, Phys. Rev. Lett. **95**, 067201 (2005).
[19] J.-I. Hong, T. Leo, D. J. Smith, and A. E. Berkowitz, Phys. Rev. Lett. **96**, 117204 (2006).
[20] M. Fecioru-Morariu, S. Rizwan Ali, C. Papusoi, M. Sperlich, and G. Güntherodt, Phys. Rev. Lett. **99**, 097206 (2007).
[21] U. Nowak, K. D. Usadel, J. Keller, P. Miltényi, B. Beschoten, and G. Güntherodt, Phys. Rev. B **66**, 014430 (2002).
[22] R. Morales, Zhi-Pan Li, J. Olamit, Kai Liu, J. M. Alameda, and Ivan K. Schuller, Phys. Rev. Lett. **102**, 097201 (2009).
[23] J. Stöhr, A. Scholl, T. J. Regan, S. Anders, J. Lüning, M. R. Scheinfein, H. A. Padmore, and R. L. White, Phys. Rev. Lett. **83**, 1862 (1999).
[24] H. Ohldag, T. J. Regan, J. Stöhr, A. Scholl, F. Nolting, J. Lüning, C. Stamm, S. Anders, and R. L. White, Phys. Rev. Lett. **87**, 247201 (2001).
[25] H. Ohldag, A. Scholl, F. Nolting, E. Arenholz, S. Maat, A. T. Young, M. Carey, and J. Stöhr, Phys. Rev. Lett. **91**, 017203 (2003).
[26] S. Roy, M. R. Fitzsimmons, S. Park, M. Dorn, O. Petracic, Igor V. Roshchin, Z.-P. Li, X. Batlle, R. Morales, A. Misra, X. Zhang, K. Chesnel, J. B. Kortright, S. K. Sinha, and I. K. Schuller, Phys. Rev. Lett. **95**, 047201 (2005).
[27] H. Ohldag, H. Shi, E. Arenholz, J. Stöhr, and D. Lederman, Phys. Rev. Lett. **96**, 027203 (2006).
[28] M. Gruyters and D. Schmitz, Phys. Rev. Lett. **100**, 077205 (2008).
[29] S. Brück, G. Schütz, E. Goering, X. Ji, and K. M. Krishnan, Phys. Rev. Lett. **101**, 126402 (2008).
[30] A. Scholl, M. Liberati, E. Arenholz, H. Ohldag, and J. Stöhr, Phys. Rev. Lett. **92**, 247201 (2004).
[31] J. Wu, J. S. Park, W. Kim, E. Arenholz, M. Liberati, A. Scholl, Y. Z. Wu, Chanyong Hwang, and Z. Q. Qiu, Phys. Rev. Lett. **104**, 217204 (2010).
[32] Q.-f. Zhan, W. Zhang, and K. M. Krishnan, Phys. Rev. B **83**, 094404 (2011).
[33] Yu. Yanson, O. Petracic, K. Westerholt, and H. Zabel, Phys. Rev. B **78**, 205430 (2008).
[34] M. Grimsditch, A. Hoffmann, P. Vavassori, H. Shi, and D. Lederman, Phys. Rev. Lett. **90**, 257201 (2003).
[35] Z. Q. Qiu, J. Pearson, and S. D. Bader, Mod. Phys. Lett. B **6**, 839 (1992).
[36] R. Mattheis and G. Quednau, J. Magn. Magn. Mater. **205**, 143 (1999).
[37] Z. Tian, C. S. Tian, L. F. Yin, D. Wu, G. S. Dong, X. F. Jin, and Z. Q. Qiu, Phys. Rev. B **70**, 012301 (2004).
[38] X. Y. Xu, L. F. Yin, D. H. Wei, C. S. Tian, G. S. Dong, X. F. Jin, and Q. J. Jia, Phys. Rev. B **77**, 052403 (2008).
[39] A. M. Nazmul, H. T. Lin, S. N. Tran, S. Ohya, and M. Tanaka, Phys. Rev. B **77**, 155203 (2008).
[40] S. T. B. Goennenwein, R. S. Keizer, S. W. Schink, I. van Dijk, T. M. Klapwijk, G. X. Miao, G. Xiao, and A. Gupta, Appl. Phys. Lett. **90**, 142509 (2007).
[41] E. Arenholz and S. O. Prestemon, Rev. Sci. Instrum. **76**, 083908 (2005).
[42] C. T. Chen, F. Sette, Y. Ma, and S. Modesti, Phys. Rev. B **42**, 7262 (1990).
[43] J. Stöhr, Y. Wu, B. D. Hermsmeier, M. G. Samant, G. R. Harp, S. Koranda, D. Dunham, and B. P. Tonner, Science **259**, 658 (1993).
[44] F. Offi, W. Kuch, L. I. Chelaru, K. Fukumoto, M. Kotsugi, and J. Kirschner, Phys. Rev. B **67**, 094419 (2003).
[45] C. Won, Y. Z. Wu, H. W. Zhao, A. Scholl, A. Doran, W. Kim, T. L. Owens, X. F. Jin, and Z. Q. Qiu, Phys. Rev. B **71**, 024406 (2005).
[46] G. Chen, J. Li, F. Z. Liu, J. Zhu, Y. He, J. Wu, Z. Q. Qiu, and Y. Z. Wu, J. Appl. Phys. **108**, 073905 (2010).
[47] G. van der Laan, E. Arenholz, R. V. Chopdekar, and Y. Suzuki, Phys. Rev. B **77**, 064407 (2008).
[48] Y. J. Tang, X. Zhou, X. Chen, B. Q. Liang, and W. S. Zhan, J. Appl. Phys. **88**, 2054 (2000).
[49] T. Zhao, H. Fujiwara, K. Zhang, C. Hou, and T. Kai, Phys. Rev. B **65**, 014431 (2001).
[50] Y.-H. Wang, C.-H. Lai, C.-R. Chang, J.-S. Yang, and C. K. Lo, J. Appl. Phys. **89**, 6603 (2001).
[51] P. Y. Yang, C. Song, B. Fan, F. Zeng, and F. Pan, J. Appl. Phys. **106**, 013902 (2009).
[52] J. Dho, M. G. Blamire, and E. O. Chi, Phys. Rev. B **72**, 224421 (2005).
[53] J. Kanamori, Prog. Theor. Phys. **17**, 197 (1957).
[54] T. C. Schulthess and W. H. Butler, Phys. Rev. Lett. **81**, 4516 (1998).
[55] J. S. Park, J. Wu, E. Arenholz, M. Liberati, A. Scholl, Y. Meng, C. Hwang, and Z. Q. Qiu, Appl. Phys. Lett. **97**, 042505 (2010).